

## IEEE Journal of Selected Topics in Quantum Electronics Vol 1, 900 (1995)

### A very convenient set-up to generate intense VUV coherent light at 125 nm with use of nonlinear effects in mercury vapor at room temperature

L. Museur<sup>1</sup>, W.Q. Zheng<sup>2</sup>, A.V. Kanaev<sup>3</sup>, M.C. Castex<sup>1</sup>.

<sup>1</sup>Laboratoire de Physique des Lasers Université PARIS-NORD

93430 Villetaneuse, France

<sup>2</sup>LURE bâtiment 209D Université PARIS-SUD

91405 Orsay cedex, France

<sup>3</sup>P. N. Lebedev Physical Institute, Academy of Sciences

Moscow, Russia

#### Abstract

Using only one dye laser, efficient generation of VUV radiation ( $10^{13}$  photons/pulse) is demonstrated at 125.140 nm and 125.053 nm by four-wave sum-frequency mixing in a room-temperature mercury vapor. The emission at 125.053 nm, which is out of two-photon resonance but near three-photon resonance, has been observed for the first time and is carefully analyzed. In particular, numerical calculations have been carried out for gaussian pump beams taking into account absorption of VUV photons and optical Kerr effect. The results of the calculations reproduce the VUV emission lineshape and power saturation effects measured in the experiment.

## I. Introduction

Methods of nonlinear optics are now successfully used in laboratories to extend the tuning range of pulsed lasers with production of intense coherent radiation in VUV spectral region.<sup>1-3</sup> This range of photon energies covers the domain of electronically excited states of small molecules and photoionization continua of the most of substances, and therefore is of high practical interest. Among different techniques of optical frequencies up-conversion, a four-wave sum-frequency mixing (*FWSPM*) in metal vapors offers advantage of high efficiency, achieved by using relatively low photon energy and intensity of pump radiation. In turn, this implies utilization of lower-cost optics and laser systems, which is highly beneficial if we consider possible applications. While two tunable lasers are necessary to generate tunable radiation, for some applications like photoionization TOF mass spectrometry, production of very intense VUV light in a narrow spectral range is needed. This last aim has stimulated the present study.

The VUV radiation intensity  $I_{\text{vuv}}$  in the low field limit and gaussian beams approximation is expressed by

$$I_{\text{vuv}} \propto N^2 I_1^2 I_2 \left| \chi^{(3)}(-\omega_{\text{vuv}}, \omega_1, \omega_1, \omega_2) \right|^2 F(b\Delta k) \quad (1)$$

where  $N$  is the number density of the nonlinear medium (Hg vapor),  $\chi^{(3)}(-\omega_{\text{vuv}}, \omega_1, \omega_1, \omega_2)$  is the third order nonlinear susceptibility,  $F(b\Delta k)$  is the phase-matching factor,  $b$  is the beam confocal parameter, and  $\Delta k = k_{\text{vuv}} - 2k_1 - k_2$  is the wave vector mismatch between the generated and the incident waves.

Among various factors which can optimize the process efficiency, it seems obvious to increase the atomic density  $N$  (which justifies the utilization of heated cells) and to enhance the nonlinear susceptibility  $\chi^{(3)}$ , mostly by a two-photon resonance. Moreover, nonlinear light production is a sensitive function of pump beam intensities. Therefore, tightly focused configuration is widely accepted in experiments to obtain intense VUV radiation. In this case, achievement of phase-matching becomes a non-trivial problem: because of the destructive interference between portions of VUV light produced before and after the focal point, the medium must be negatively dispersive at the frequency of the generated VUV. Finally, the intensities  $I_1$  and  $I_2$  may be increased till saturation phenomena start to appear.

Since two decades, several groups, Stoicheff et al.,<sup>6</sup> Hilbig et al.,<sup>7</sup> Mahon et al.,<sup>8,9</sup> and Smith et al.,<sup>10-12</sup> have studied in detail and demonstrated that, among the metallic

species, mercury vapor is an appropriate nonlinear medium to produce the 105-200 nm VUV light. In these first studies, as in more recent works,<sup>13-15</sup> the mercury is heated (typically to 200° C) in a specially-designed cell in presence of a buffer gas (He or Ar), and a two-photon resonance enhancement is used to reach a conversion efficiency up to 0.5%. The experimental arrangement is usually composed of two dye lasers pumped by the second harmonic of Nd:YAG laser. One dye laser, frequency doubled ( $\omega_1$ ), is adjusted on one of allowed two-photon transitions of atomic mercury, while the other dye laser, with a tunable frequency ( $\omega_2$ ), allows the production of tunable VUV coherent radiation at  $\omega_{\text{vuv}} = 2\omega_1 + \omega_2$ . (The difference frequency mixing process, which offers broader tuning, has also been considered in these studies).

Summarizing, the low-energetic performance of Hg-vapor based coherent frequency up-conversion ( $P_{\text{pump}} \leq 100$  kW) is now well understood. Unfortunately, this is not the case of high pump intensities, where saturation processes appear. Characterization of the last case is of importance, since for many applications VUV power of  $\geq 10$   $\mu\text{J}/\text{pulse}$  and even  $\sim 1$  mJ is highly desirable. Metallic and particularly mercury vapors as nonlinear media are well suited to generate VUV radiation below a cut-off of the short-wavelength LiF optics ( $\leq 11.8$  eV) by a two-photon enhanced *FWSFM* process. However, they are more difficult to handle requiring heat-pipe techniques to reach the conditions of sufficient vapor pressure, together with homogeneity of the nonlinear medium to satisfy phase-matching conditions.

On the basis of these results, we investigated the possibilities offered by mercury vapor for the production of VUV radiation. With the purpose to set up an intense pulsed VUV source, not necessary tunable, but, reliable and easy to handle, we have probed an original solution. In the spectral domain of 125 nm, a sum frequency mixing scheme offers an enhanced efficiency even using only one tunable source of laser radiation ( $\omega_{\text{dye}}^{-1} \simeq 626$  nm). This is due to a nearly double resonance condition in the nonlinear medium: the two-photon resonance ( $6s^1S_0 \rightarrow 7s^1S_0$ ) for doubling dye laser frequency ( $\omega_1$ ), and the one-photon resonance ( $6s^1S_0 \leftarrow 9p^1P_1$ ) for the VUV one ( $\omega_{\text{vuv}} = 2\omega_1 + \frac{1}{2}\omega_1$ ). Under these conditions, pulses of VUV radiation of  $10^{13}$  photons have been obtained in pure mercury vapor at room temperature (which corresponds to atomic density as low as  $4 \cdot 10^{13}$  at/cm<sup>3</sup>) by using a Nd:YAG laser pumped dye laser. Two intense emissions are generated respectively, at 125.140 and 125.053 nm when scanning the dye laser wavelength, as shown by fig.1. The scheme of the nonlinear processes is shown in fig.2.

While the 125.140 nm emission has been reported more than one decade ago,<sup>8</sup> when

the doubled dye laser ( $\omega_1$ ) is adjusted on the two photon resonance  $6s^1S_0 \rightarrow 7s^1S_0$  (fig.2a), the second emission at 125.053 nm, observed for the first time, is nearly resonant with the  $6s^1S_0 \leftarrow 9p^1P_1$  transition and  $\sim 44 \text{ cm}^{-1}$  above the two photon resonance (fig.2b). Both emission lines are of interest for several reasons.

(i) Surprisingly, as noted one decade ago by Mahon et al.,<sup>9</sup> the 125.140 nm emission is observed in a spectral region of positive dispersion of nonlinear medium, where phase-matching is not satisfied under tight-focusing conditions. Until the present, the reason for efficient VUV generation at 125.140 nm has been an open question.

(ii) On the contrary, sum generation at 125.053 nm corresponds to a region of negative dispersion. It may provide a straightforward example to check, experimentally and theoretically various parameters of *FWFSM* processes which can be optimized to yield the maximum attainable conversion efficiency.

(iii) 125.140 nm and 125.053 nm emission lines are expected to undergo different kinds of dominant saturation processes, which are interesting to follow. While a two-photon absorption could limit the first line production efficiency, the detuning from the resonance would change the nature of saturation and its onset. Here modification of the refractive index of nonlinear medium by the intense visible light may destroy phase-matching (optical Kerr effect). It is worth noting, that the off-resonance conditions offer the possibility of investigating this phenomenon, which is greatly suppressed in the resonant case. For the two-photon resonant situation, it is the imaginary part of a third order nonlinear susceptibility  $\chi^{(3)}$  that gives rise to the two-photon absorption and modifies the physical characteristics of the nonlinear medium, whereas for the non-resonant situation, it is the real part of a  $\chi^{(3)}$  which causes the intensity-dependent change of the refractive index and therefore introduces another type of modification. In this case, the first line intensity is expected to be restricted with respect to the UV pump beam (doubled dye laser output) and the second, to the visible beam (fundamental dye laser frequency).

The results concerning the development of the intense VUV coherent source are presented in this paper, with a discussion about the conversion efficiencies and saturation processes. Although experimental results are given for both 125.140 nm and 125.053 nm emissions, we shall concentrate mostly on the 125.053 nm line. The 125.140 nm line will be discussed in a foregoing article. The detailed study of the 125.053 nm emission, presented in this paper, is based on: (a) quantitative experimental determinations of the VUV profile and intensity as a function of the UV and visible pump beam intensities, and (b) theoretical calculations to account for the experimental results. At the end we shall

demonstrate an application of the VUV source to a cluster beam experiment.

## II. Experimental arrangement and results

Because of the experimental simplification which results from the use of a mercury cell at room temperature, we have focused our attention on an experimental optical arrangement which allows precise measurements of the VUV intensity as a function of the UV and visible pump beam intensities.

The schematic diagram of our experiment is given in fig.3. A commercial pulsed Nd:YAG laser (Quantel YD 481, 20 Hz, 10 ns, 200 mJ at 532 nm) is used to pump a Quantel TDL 50, pulsed dye laser, working with mixed DCM and Rhodamine 640 in methanol. The tunable laser beam around 626 nm ( $\approx 20$  mJ/pulse, spectral linewidth of about  $0.1 \text{ cm}^{-1}$ ) is sent into an autotracker system (UVT.1A Quantel) to produce the second-harmonic beam (313 nm,  $\approx 4$  mJ/pulse) through an angle-tuned KDP crystal coupled with a quartz compensator which keeps the output beams in a fixed direction. Behind the tracking system, a zig-zag device, composed of two dichroic mirrors ( $R_{Max}$  for 308 nm) and two right angle suprasil quartz prisms, is used to split and recombine two collinear UV and visible laser beams. With such a specific arrangement it is possible to attenuate independently the UV or the visible beam by introducing a neutral filter in one part of the zig-zag and to perform precise measurements of the VUV power as a function of each of the pump beam powers separately. The neutral filter used is a home-made cell (length  $\approx 4$  cm) with two parallel quartz windows, containing water in which some drops of ink are diluted, thus allowing a variable attenuation of laser light intensity over several decades. The temporal lag introduced between two beams with such an arrangement is negligible and the temporal coincidence of the laser pulses is thus well conserved. The beams ( $D \approx 0.5$  cm) are then focused by an achromatic lens ( $f = 28$  cm) into the middle 23 cm long, stainless-steel, Hg vapor cell at room temperature ( $N_{Hg} \approx 4 \cdot 10^{13}$  at/cm<sup>3</sup> at 20°C). The cell, which can be vacuum pumped, is closed at the entrance by a quartz window and at the exit by a plano-convex LiF lens ( $f = 10$  cm at 125 nm) which collimates the VUV beam into a parallel beam of 1 mm diameter. A MgF<sub>2</sub> Pellin-Broca prism is used behind the mercury cell to separate the intense red (626 nm) and UV (313 nm) beams from the VUV beam. The VUV beam is then sent to either a scatterer (a plane rough stainless steel surface) to be detected at right angle by a CsI solar-blind photomultiplier (PMT), or to a visible PMT coated with a sodium salicylate phosphor. To record VUV profiles when scanning the dye laser frequency or to detect pulsed waveforms, we used

either a boxcar averager with an integration time of 1 second or a 250 MHz Hewlett Packard 54510A digitizing oscilloscope.

With the use of a sodium salicylate coated visible photomultiplier, absolute VUV photon measurements were obtained by comparing the signal of the VUV beam with that of the UV beam. The constant relative quantum yield of the sodium salicylate throughout a broad spectral range from 100 nm to 350 nm makes it favorable for intensity calibrations (see e.g. in<sup>16</sup>). We have introduced a glass plate (cut-off at  $\sim 400$  nm) before the visible PMT with the face coated by a thin freshly prepared slab of the phosphor ( $\sim 100$   $\mu\text{m}$ ) toward the incident radiation. The system has been carefully calibrated to guarantee the linearity of the photomultiplier response and the rejection of any UV/visible fluorescence and stray lights with use of an additional 125 nm interference filter. Under these conditions, the VUV intensity is just equal to the known UV intensity multiplied by an attenuation factor and the PMT signals ratio. Using 16 mJ visible and 4 mJ UV input laser powers, we have measured  $\sim 10^{13}$  photons/pulse ( $\sim 20$   $\mu\text{J}$ /pulse) for the stronger one of two VUV emissions: the intensity peak at 125.053 nm being roughly 1/3 of that at 125.140 nm. Our value of  $10^{13}$  photons/pulse is of the same order of magnitude when compared to other measurements in Hg vapor,<sup>9,7</sup> but we used a much simpler experimental system with only one dye laser and a non-heated Hg cell.

In order to characterize more quantitatively our VUV generation, we have studied the VUV intensity dependence with respect to the pump beam intensities. In the case of 125.140 nm line, when the visible intensity is kept constant and the UV intensity changes, we have observed, as expected from (1), a quadratic dependence only when  $E_{\text{uv}} < 0.5$  mJ/pulse: a fit of our experimental points gives  $I_{\text{vuv}} \propto I_{\text{uv}}^{2.08}$ . At higher UV intensity, we have detected principally a linear variation of VUV intensity:  $I_{\text{vuv}} \propto I_{\text{uv}}^{1.07}$  (fig.4). On the other hand, we have observed a nearly linear dependence of the VUV intensity with the visible intensity ( $I_{\text{vuv}} \propto I_{\text{vis}}^{0.82}$ ) when the UV power is kept constant.

On the contrary, for the new emission at 125.053 nm, we didn't observe any saturation phenomena when the UV intensity increases. In the whole UV intensity range accessible with our dye laser, we have observed a quadratic dependence of the VUV intensity,  $I_{\text{vuv}} \propto I_{\text{uv}}^{1.84}$  (fig.5). On the other hand, when the visible intensity rises and the UV intensity is fixed, the VUV intensity deviates progressively from linear dependence, as shown in fig.6. Moreover, in contrast to the symmetrical profile of the emission observed at 125.140 nm, the lineshape of the 125.053 nm emission is quite different (see fig.7). In fact, for this band, intensity enhancement results from a three-photon resonance rather than from a

two-photon resonance and, therefore, the emission profile is expected to be influenced by an absorption.

### III. Numerical simulations and discussion

Without saturation effects the VUV intensity dependence would be proportional to  $I_1^2 I_2$ , according to Eq.(1). In fact, for low incident energy we do observe such a variation, but it is clear that the VUV intensity doesn't follow this law when the input intensities are sufficiently high. Besides, the two VUV emissions behave differently. That at 125.140 nm, deviates from the usual law given by Eq.(1) when the UV power increases above 50 kW, whereas the emission at 125.053 nm, displays saturation only when visible power is  $\geq 1$  MW. Nevertheless this difference is not completely surprising since these emissions are generated in two different physical situations. Below we shall discuss the two emissions separately.

#### A. 125.140 nm emission

The 125.140 nm emission is obtained by two-photon resonant *FWSPM*. Under these conditions the efficiency of the conversion process is expected to be limited principally by the two-photon absorption as shown by Puell et al.<sup>17</sup> in the case of third harmonic generation. In the small-signal region the two photon absorption rate for the  $6s^1S_0 \rightarrow 7s^1S_0$  transition can be expressed as  $2.3 \cdot 10^{-6} (P/A)^2$ , where  $P/A$  is the UV power density in W/cm<sup>2</sup>.<sup>9</sup> Therefore, with our experimental conditions ( $P = 6$  MW,  $A = b\lambda_1/2 \approx 2.8 \cdot 10^{-3}$  cm<sup>2</sup>, and the confocal parameter  $b = 1.9$  cm measured for the UV beam), substantial quantity of Hg atoms ( $\sim 50\%$ ) are in the  $7s^1S_0$  state in the region of the beam waist, where the process of frequency conversion generally takes place. The VUV intensity would no longer be proportional to the square of the density of Hg ground-state atoms but to the square of population difference  $N^2 \cdot (\rho_{6s^1S_0} - \rho_{7s^1S_0})^2$ , where  $\rho_i$  is the fractional population of level  $i$ .<sup>18</sup> Consequently, the VUV generation efficiency will decrease. In turn, the  $7s^1S_0$  level population induces a one-(UV)photon photoionization, which reduces the concentration of mercury atoms and contributes to the power saturation. Another point of speculation is that the  $7s^1S_0$  level population changes the phase-matching conditions directly or by enhancement of the nonlinear medium ionization. Additionally, cascade radiative decay from the  $7s^1S_0$  level through the  $6p^1P_1$  results in the parametric resonance generation at 1.014  $\mu\text{m}$  and 184.96 nm.<sup>8</sup> A more quantitative analysis of the 125.140 nm

emission requires taking into account all of these processes.

Now we would like to discuss briefly the reason for the efficient 125.140 nm light production. In fact, the restrictions mentioned above are put forward to account for the reduction of efficiency of the nonlinear process, but not to explain its appearance. Apparently, the process doesn't start from the "cold" mercury,  $\text{Hg}(6s^1S_0)$ . The phase-matching condition is not satisfied for the 125.140 nm generation, which is produced in a region of positive dispersion of mercury vapor (low energy side of the  $9p^1P_1 \leftarrow 6s^1S_0$  transition). In disagreement with Hilbig et al.,<sup>7</sup> who have reported disappearance of VUV light production by *FWSPM* in the region of positive dispersion (125.056-125.48 nm) at Hg pressures as low as 0.17 torr, we observe a strong signal at  $p_{\text{Hg}} \simeq 0.0012$  torr. We do not heat the mercury and therefore we could not put forward density gradients to explain the VUV generation effect.<sup>7</sup> (The disappearance of the VUV signal in the experiments of Hilbig et al.<sup>7</sup> could be related to the presence of a buffer gas. We observe indeed a strong suppression of the VUV emission when helium is added.<sup>19</sup>) In our opinion, the effect is due to the presence of a strong UV field adjusted to the  $7s^1S_0 \leftarrow 6s^1S_0$  two-photon transition. Population of the  $7s^1S_0$  excited level increases the refractive index of mercury vapor at the visible frequency  $\omega_{\text{dye}} = \frac{1}{2}\omega_1$ , which improves the phase-matching (detuning  $\delta\omega$  from the  $9p^1P_1$  level for both VUV and visible frequencies conserves phase automatically). The contribution from the ionization continuum to the nonlinearity and dispersion of  $\text{Hg}(6s^1S_0)/\text{Hg}^*(7s^1S_0)$  vapor at frequencies  $\omega_1$  and  $\omega_{uv}$  is not yet clear to us. Higher order nonlinear susceptibilities  $\chi^{(n)}$  ( $n > 3$ ) can participate too. Calculations to account for these contributions are in progress.

Finally, we would like to point out two consequences, which may result from this proposal. (i) The first is that because of the direct one(UV)-photon photoionization losses from the  $7s^1S_0$  level, the VUV intensity can be found linearly dependent on the UV intensity. This is in agreement with our experimental results, and the same effect has been reported earlier in experiments using heated mercury vapor with a buffer gas.<sup>7,8</sup> (ii) The second is that the generation of the 125.140 nm line (if it is a process of *FWSPM*) would display a threshold character. Really, if we suppose that phase-matching conditions are satisfied only when  $[\text{Hg}^*(7s^1S_0)]/[\text{Hg}(6s^1S_0)] = \gamma \geq \gamma_{thr}$ , where  $\gamma$  is a UV intensity dependent factor, the VUV coherent field will appear only at  $I_{uv} \geq I_{uv}(\gamma_{thr}) \equiv I_{thr}$ . This could be the subject of an experimental verification. A more precise description of the 125.140 nm emission will be given in a foregoing article.

## B. 125.053 nm emission

The conditions of observation of the 125.053 nm emission are completely different for several reasons.

(i) The emission is observed in a region of negative dispersion (blue wing of the  $9p^1P_1$  level) and can be analyzed in the framework of the usual phase-matching theory developed for focused Gaussian beams.<sup>20,21</sup>

(ii) In the vicinity of the  $9p^1P_1 \leftarrow 6s^1S_0$  dipole allowed transition, which enhances the nonlinear process, the generated VUV photons can be absorbed by the Hg vapor. This process contributes to the spectral shift of the emission line (from the exact three-photon resonance:  $\omega_{\text{vuv}} = 2\omega_1 + \omega_2 \neq \omega_{9p^1P_1}$ ), which depends on the width  $\Gamma_{9p^1P_1}$  of the  $9p^1P_1$  level.

(iii) This emission line is not generated through two-photon resonance and the saturation effect cannot be explained by two-photon absorption. In the non-resonant case, the optical Kerr effect can be the most important limiting process. We have associated the observed saturation of VUV intensity with a change of refractive index induced by the visible light.

These conclusions have been verified with numerical simulations of the emission line-shape as well as with the VUV intensity variation as a function of the visible intensity. In order to simplify these calculations we have used two main assumptions. (a) We characterize both visible and UV pump laser beams by the smaller confocal parameter  $b = 1.9$  cm, which has been measured for our UV beam. (b) Different factors contribute to the broadening of the  $9p^1P_1$  level, which appears in the third-order nonlinear susceptibility term. In addition, the situation is complicated by the contribution of six naturally abundant mercury isotopes. In fact, the isotopic structure of mercury is narrow ( $\delta\omega_{\text{isotop.}} \sim 0.4$  cm<sup>-1</sup>),<sup>22,11</sup> and the splitting between the different isotopic sublevels is smaller than the Stark broadening induced by the VUV light in our experimental conditions. Really, the Stark broadening can be evaluated from the known dipole moment of the  $9p^1P_1 \rightarrow 6s^1S_0$  transition (see below) using the relation<sup>23</sup>  $\Delta\omega_S = 3.3 \cdot 10^{-4} (I_{\text{vuv}})^{1/2}$  (where  $\Delta\omega_S$  is expressed in cm<sup>-1</sup> and  $I_{\text{vuv}}$  in W/cm<sup>2</sup>). The estimation gives a value of  $\sim 0.6$  cm<sup>-1</sup> in our experimental conditions. Therefore, one cannot resolve the isotopic structure, and we have neglected it in our simulations.

The VUV power is given by Eq.(1). In this equation both the nonlinear susceptibility  $\chi^{(3)}(-\omega_{\text{vuv}}, \omega_1, \omega_1, \omega_2)$  and the phase-matching function  $F(b\Delta k)$  are wavelength dependent and need to be written explicitly. In our specific case the  $\chi^{(3)}$  term can be factored

as

$$\chi^{(3)}(-\omega_{\text{vuv}}, \omega_1, \omega_1, \omega_2) \propto \left[ \omega_{9p^1P_1} - \omega_{\text{vuv}} - i\Gamma_{9p^1P_1} \right]^{-1} \times \left[ \omega_{7s^1S_0} - 2\omega_1 \right]^{-1} \quad (2)$$

For the phase-matching function we shall use the expression given by Lago et al.<sup>21</sup> in the case of a tight-focussed gaussian beam in a uniform nonlinear medium situated between the planes  $z = -L/2$  and  $z = L/2$

$$F(b\Delta k) = \left| \frac{4}{b} \int_{-L/2}^{+L/2} \frac{\exp i \left[ \int_z^{L/2} k_{\text{vuv}} dz'' + \int_{-L/2}^z (2k_1 + k_2) dz'' \right]}{\left[ 1 + i \frac{2}{b} z \right]^2} dz \right|^2 \quad (3)$$

where  $b$  is the beam confocal parameter. We have taken into account the effect of absorption of the generated VUV light by introducing the complex wave vector

$$k_{\text{vuv}} = \frac{2\pi}{\lambda_{\text{vuv}}} n_{\text{vuv}} + iN \frac{\sigma_{\text{vuv}}}{2} \quad (4)$$

where  $\sigma_{\text{vuv}}$  is the absorption cross section. Finally, we have taken into account a correction term  $\delta n_{\text{vuv}}$  to the medium refractive index at the VUV frequency induced by intense pump radiation. It is responsible for the optical Kerr effect. Among different contributions, the most important is that induced at the VUV frequency by the visible light intensity, which can be expressed as<sup>18</sup>

$$\delta n_{\text{vuv}} = \frac{3N}{4} \frac{\mathcal{R}e \left[ \chi_K^{(3)}(-\omega_{\text{vuv}}; \omega_2, -\omega_2, \omega_{\text{vuv}}) \right]}{\varepsilon_0 c n_2 n_{\text{vuv}}} \frac{I_{20}}{\left[ 1 + 4 \left( \frac{z}{b} \right)^2 \right]} \quad (5)$$

where  $I_{20}$  is the intensity at the focal point, and (we keep only the principal resonant term)

$$\chi_K^{(3)}(-\omega_{\text{vuv}}; \omega_2, -\omega_2, \omega_{\text{vuv}}) = \frac{1}{6\hbar^3 \varepsilon_0} \frac{|\langle 9p^1P_1 | \mu | 7s^1S_0 \rangle \langle 9p^1P_1 | \mu | 6s^1S_0 \rangle|^2}{(\omega_{7s^1S_0} - 2\omega_1) (\omega_{9p^1P_1} - \omega_{\text{vuv}} - i\Gamma_{9p^1P_1})^2} \quad (6)$$

with  $\langle 9p^1P_1 | \mu | 7s^1S_0 \rangle = 0, 4454693 \text{ ea}_0$  and  $\langle 9p^1P_1 | \mu | 6s^1S_0 \rangle = 0, 3039320 \text{ ea}_0$ .<sup>12</sup> Finally we put (4) and (5) into relation (3) and integrate over  $z''$  to obtain the final expression of the phase-matching function.

In the equations given above, refractive indices  $n_i$  and the absorption cross-section  $\sigma_{\text{vuv}}$  can be obtained from the oscillator strengths given by Smith et al.<sup>12</sup> Except for the

value of  $\Gamma_{9p^1P_1}$ , all terms in the previous expressions are known or calculable. Therefore, the linewidth  $\Gamma_{9p^1P_1}$  has been taken as the only free parameter to fit the VUV emission lineshape. The best fit with  $\Gamma_{9p^1P_1} = 1.05 \text{ cm}^{-1}$  is shown in fig.7. In fact, as we mentioned above, this value cannot be considered as a pure linewidth of the  $9p^1P_1$  level, but rather as an effective parameter which characterizes the integral contribution of mercury isotopes. We obtain (see the above discussion of the line broadening factors) that  $\Delta\omega_S + \delta\omega_{\text{isotop.}} = 1.0 \text{ cm}^{-1} \simeq \Gamma_{9p^1P_1}$ , which proves our assumption (b). In view of this result one cannot expect to gain in VUV generation efficiency by using an isotopically pure mercury. Because of the lines overlapping at high laser intensity, all isotopes contribute to the VUV signal build-up.

Our calculation, which reproduces correctly the variation of the VUV intensity in the blue wing of the  $9p^1P_1$  level, are not valid in the red wing where the dispersion is positive. Here appreciable VUV generation occurs, which is in quantitative disagreement with the calculations, which predict only a very small signal. In order to explain the presence of a small VUV signal in the low energy side of  $9p^1P_1$  level we have calculated this same lineshape with the more general expression of the phase-matching function given by Hilber et al.<sup>24</sup> In this expression the specific confocal parameter of each laser beam is taken into account. Nevertheless we have observed almost no difference between the two results. As expected, the VUV signal reaches its maximum when the laser frequency is shifted by  $\sim 1.0 \text{ cm}^{-1}$  from the exact three-photons resonance. This is natural effect of the VUV light absorption. In fact, the absorption coefficient in (4) depends on the laser beam intensity and, hence, on the propagation coordinate 'z' in our tight-focusing experimental conditions. We have introduced a power-dependent absorption of the VUV beam in the mercury vapor, phenomenologically in our calculations. This has resulted in the quantitative agreement with the experimental observations.

With the linewidth  $\Gamma_{9p^1P_1}$  obtained from the lineshape fit, we have calculated the variation of the VUV intensity when the visible intensity increases. The result of this calculation is shown in fig.6 by a solid line. It is in a good agreement with the experimental observation. The consistency of the results allows us ultimately to assign the dominant factor, which governs the saturation of the VUV coherent light generation at 125.053 nm, to the optical Kerr effect induced by the visible light. The increment of the refractive index is important when visible intensity is high, and it "damages" progressively the phase-matching conditions.

Summarizing, we like to point out the possibility of an increase of the VUV generated

power. In fact, it is not clear, which of the two emissions is more promising in this connection. Saturation effects have been found in respect to the UV pump radiation (the 1st line: 125.140 nm) and to the visible radiation (the 2nd line: 125.053 nm). Those saturation mechanisms are different. But as we have demonstrated the VUV intensity continues to grow for both lines in the  $\geq 1$  MW pump domain region:  $I_{\text{vuv}}^{(1st)} \propto I_{\text{uv}} \cdot I_{\text{visible}}$  and  $I_{\text{vuv}}^{(2nd)} \propto I_{\text{uv}}^2$ , respectively. This is an "encouraging" fact. On this basis we expect further progress in the VUV generation efficiency.

### C. Application to cluster-beam experiments.

The first application of our intense VUV source ( $h\nu \simeq 10$  eV) has concerned a cluster beam experiment devoted to the problems of electronic energy acquisition, storage and disposal in many-body and finite-size systems. The rare-gas clusters weakly bound by Van der Waals forces in their ground-state configuration appear to be a good model to study how individual atomic properties evolve to the condensed phase properties. Two peculiarities are known which create problems to develop such experiments. (i) Absorption bands of rare-gas clusters lie in the VUV spectral region. (ii) Because of low concentration, cluster beams are highly transparent, at least at small particle sizes. Currently, these experiments are carried out only at synchrotrons.<sup>25</sup> Synchrotron radiation (SR) with inherently high repetition rate ( $\nu \geq 1$  MHz) allows the use of a very sensitive detection technique of time-correlating single-photon counting (TCSPC).

Intense excitation with our VUV radiation offers the possibility to measure real-time fluorescence decay directly by using VUV-sensitive fast photomultipliers. In our experiment we have investigated fluorescence decay of  $Kr_n$  clusters ( $n = 2-2000$ ) produced in the supersonic expansion of krypton gas through a nozzle ( $d=100 \mu$ ,  $\theta/2=15^\circ$ ), with excitation at 125.140 nm. Excitation at this frequency corresponds approximately to the energetic position of the lowest metastable  $^3P_2$  atomic level of atomic krypton, and to the first surface exciton of the solid. Supplementary to the low concentration of clusters, the absorption coefficient at  $\sim 125$  nm is also very low. Nevertheless, we have observed a strong fluorescence signal. Typical fluorescence decay curves are shown in fig.8. The shapes of these curves undergo modifications with cluster size: multi-exponential for small krypton clusters ( $n \leq 30$ ); single-exponential for middle sizes ( $n \sim 10^2$ ); two dominant decay components for large clusters ( $n \sim 10^3$ ). A decay time of 410(15) ns has been obtained in the spectral region of the so-called second continuum ( $\lambda_{\text{fluor}} \simeq 145$  nm) for  $n \sim 10^2$ .

This is the first application of our VUV source in a cluster beam experiment. We do not intend to discuss the scientific merit of the results,<sup>26</sup> but rather we would like to demonstrate the performance of our VUV source. For the reason of high energy/pulse and low repetition rate, our VUV source is highly beneficial for studies which involve weak excitation bands and long  $\mu s$ -decays. In this respect it serves to be a supplementary tool to SR (time scale of SR-studies is generally limited by  $\nu^{-1} \leq 1 \mu s$ ). As we see from fig.8, in this specific domain of experimental conditions the excellent signal-to-noise ratio of  $\geq 10^3$  is conserved, which is characteristic of best measurements using TCSPC.

#### IV. Conclusion.

By focusing the fundamental beam of a dye laser ( $\sim 626$  nm) together with its second harmonic ( $\sim 313$  nm) into room temperature mercury vapor, we have observed two intense VUV emissions at 125.140 nm and 125.053 nm ( $I_{\text{vuv}} \simeq 10^{13}$  photons/pulse), ascribed to a four-wave sum-frequency mixing process. We have shown, that different saturation mechanisms govern those powers. The emission at 125.053 nm, generated near three-photon resonance is observed for the first time. Numerical simulations with the approximation of gaussian profiles of pump beam intensities, and taking into account both the VUV light absorption and optical Kerr effect, allow us to reproduce its emission lineshape and power saturation. Further development of the VUV source (desirable power level is  $\sim 1$  mJ/pulse) is under way, which apparently will extend applications of this conveniently operable system.

## References

- <sup>1</sup>S.C. Wallace, "Nonlinear optics and laser spectroscopy in the vacuum ultraviolet" in *Advances in Chemical Physics*, vol. 47, pp. 153-157, 1981.
- <sup>2</sup>C.R. Vidal, "Four-Wave Frequency Mixing in Gases" in "Tunable Lasers" Springer-Verlag Berlin Heidelberg, pp. 57-113, 1987.
- <sup>3</sup>B.P.Stoicheff, "Generation of coherent and tunable ultraviolet radiation by scattering processes", *Pure and Appl. Chem*, vol. 59, pp. 1237-1246, 1987.
- <sup>4</sup>K.D. Bonin and T.J. McIlrath, "Generation of tunable coherent radiation below 1000 Å by four-wave mixing in krypton", *J. Opt. Soc. Am. B*, vol. 2, pp. 527-533, 1985.
- <sup>5</sup>R. Hilbig, G. Hilber, A. Lago, B. Wolff and R. Wallenstein, "Tunable coherent radiation generated by nonlinear optical frequency conversion in gases", *Comments. At and Mol. Phys*, vol. 18, pp. 157-180, 1986.
- <sup>6</sup>P.R. Herman, P.E. LaRocque, R.H. Lipson, W. Jamroz and B.P. Stoicheff, "Vacuum ultraviolet laser spectroscopy III: laboratory sources of coherent radiation tunable from 105 to 175 nm using Mg, Zn and Hg vapors", *Can. J. Phys.*, vol. 63, pp.1581-1588, 1985.
- <sup>7</sup>R. Hilbig and R. Wallenstein, "Resonant sum and difference frequency mixing in Hg", *IEEE J. Quantum Electron.*, vol. QE-19, pp. 1759-1770, 1983.
- <sup>8</sup>F.S. Tomkins and R. Mahon, "High-frequency four wave sum and difference mixing in Hg vapor", *Opt. Lett.*, vol. 6, pp. 179-181, 1981.
- <sup>9</sup>R. Mahon and F.S. Tomkins, "Frequency up-conversion to the VUV in Hg vapor", *IEEE J. Quantum Electron.*, vol. QE-18, pp. 913-920, 1982.
- <sup>10</sup>A.V. Smith, W.Alford and G.R. Hadley, "Optimization of two -photon resonant four-wave mixing : application to 130.2 nm generation in mercury vapor", *J.Opt. Soc. Am. B.*, vol. 5, pp. 1503-1519, 1988.
- <sup>11</sup>A. V. Smith, G. R. Hadley, P. Esherick, W. J. Alford, "Efficient of two-photon resonant frequency conversion in mercury : the effects of amplified spontaneous emission", *Optics lett.*, vol. 12, pp. 708-710, 1987.

- <sup>12</sup>A. V. Smith, W. J. Alford, "Vacuum ultraviolet strengths of Hg measured by sum-frequency mixing", *Phys. Rev. A*, vol. 33, pp. 3172-3180, 1986; "Practical guide for 7s resonant frequency mixing in mercury: generation of light in the 230-185- and 140-120-nm ranges", *J.Opt.Soc.Am.B.*, vol.4, pp.1765-1770, 1987.
- <sup>13</sup>K. Tskiyama, M. Tsukakoshi and T. Kasuya, "Saturation and detuning effects of pump waves in VUV generation by resonant sum frequency mixing in Hg", *Japan. J. Appl. Phys.*, vol. 27, pp. 1552-1553, 1988.
- <sup>14</sup>M. Yen, P.M.Johnson and M.G. White, "The vacuum ultraviolet photodissociation of the chlorofluorocarbons. Photolysis of CF<sub>3</sub>Cl, CF<sub>2</sub>Cl<sub>2</sub> and CFCl<sub>3</sub> at 187, 125 and 108 nm.", *J.Chem. Phys.*, vol. 99, pp. 126-139, 1993.
- <sup>15</sup>T. Glenewinkel-Meyer, J.A. Bartz, G.M.Thorson and F.F.Crim, "The vacuum ultraviolet photodissociation of silane at 125.1 nm", *J. Chem. Phys.*, vol. 99, pp. 5944-5950, 1993.
- <sup>16</sup>V.S.Zuev, A.V.Kanaev, L.D.Mikheev. "Measurements of absolute luminescence quantum efficiency of mixtures of Cl<sub>2</sub> with Ar, Kr, and Xe excited by vacuum ultraviolet radiation", *Sov.J.Quantum Electron.*, vol. 14, pp. 242-248, 1984.
- <sup>17</sup>H. Puell, H. Scheingraber and C.R.Vidal, "Saturation of resonant third-harmonic generation in phase-matched systems", *Phys. Rev A*, vol. 22, pp. 1165-1178, 1980.
- <sup>18</sup>See for exemple: D.C. Hanna, M.A. Yaratich and D. Cotter in "Nonlinear optics of free atoms and molecules", Springer Series in Optics Sciences, Vol. 17, 1979.
- <sup>19</sup>L.Museur. Thèse, Université Paris-Nord, Villetaneuse, France.
- <sup>20</sup>G. C. Bjorklund, " Effects of third-order nonlinear processes in isotropic media", *IEEE J. Quantum Electron.*, vol QE-11, pp. 287-296, 1975.
- <sup>21</sup>A. Lago, G. Hilber, R. Wallenstein, "Optical frequency conversion in gaseous media", *Phys. Rev. A*, vol 36, pp. 3827-3836, 1987.
- <sup>22</sup>S. Gerstenkorn, J. J. Labarthe, J. Vergès, "Fine and hyperfine structure and isotope shifts in the arc spectrum of mercury", *Phys. Scr.*, vol. 15, pp. 167-172, 1977.
- <sup>23</sup>N. B. Delone, V. P. Kraïnov, "Fundamentals of nonlinear optic of atomic gases", John Wiley & Sons, pp. 22, 1988.

<sup>24</sup>G. Hilber, D. J. Brink, A. Lago, R. Wallenstein, "Optical-frequency conversion in gases using Gaussian laser beams with different confocal parameters", *Phys. Rev. A.*, vol. 38, pp. 6231-6239, 1988.

<sup>25</sup>T.Möller. *In* A.Ding (Ed.) : "Progress and Applications of Synchrotron Radiation to Molecules and Clusters", Cambridge Univ.Press, to be published.

<sup>26</sup>Article in preparation.

## Figures

FIG. 1. VUV emission lines observed by scanning dye laser wavelength between 625 and 627 nm.

FIG. 2. Schemes of nonlinear sum-frequency generation in Hg vapor: 125.140 nm (a), and 125.053 nm (b) lines.

FIG. 3. Experimental set-up.

FIG. 4. Variation of the VUV intensity  $I_{vuv}$  at 125.140 nm with respect to the UV intensity  $I_1$  (visible intensity is constant  $E_{vis} = 16$  mJ).

FIG. 5. Variation of the VUV intensity  $I_{vuv}$  at 125.053 nm with respect to the UV intensity  $I_1$  (visible intensity is constant  $E_{vis} = 16$  mJ).

FIG. 6. Variation of the VUV intensity  $I_{vuv}$  at 125.053 nm with respect to the visible intensity  $I_2$  (UV intensity is constant  $E_{uv} = 4$  mJ). The dotted line shows a linear extrapolation.

FIG. 7. Spectral lineshape of the 125.053 nm emission. The result of calculation using the  $9p^1P_1$  level linewidth of  $1.05 \text{ cm}^{-1}$  is shown by a solid line.

FIG. 8. Fluorescence decay curves of  $Kr_n$  clusters excited with the VUV radiation at 125.140 nm.

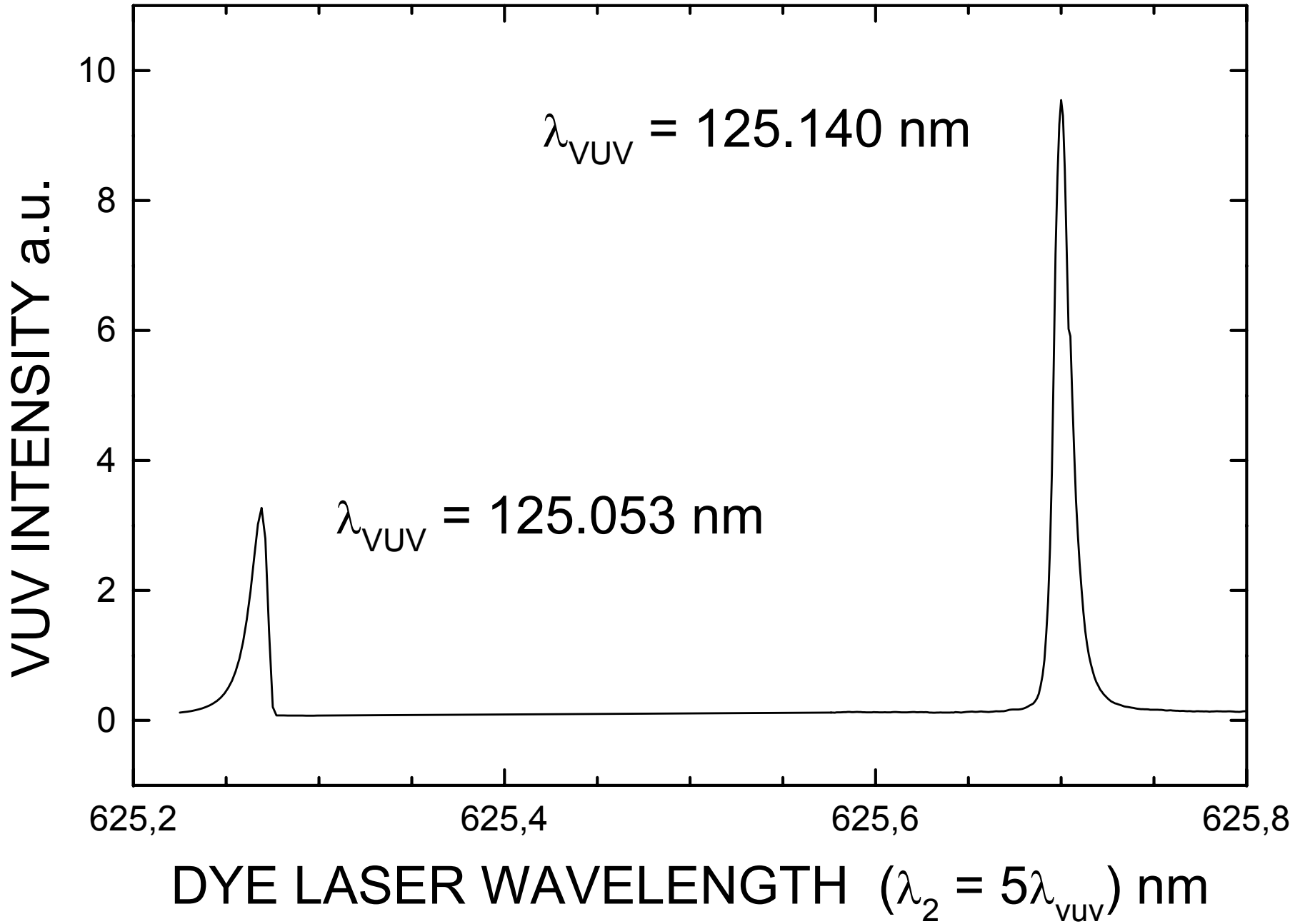
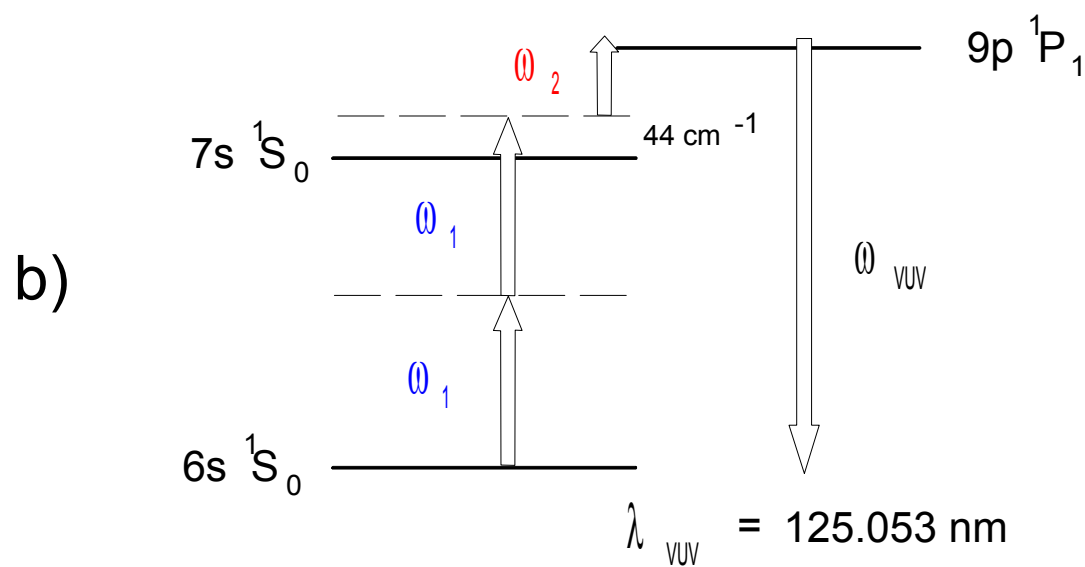
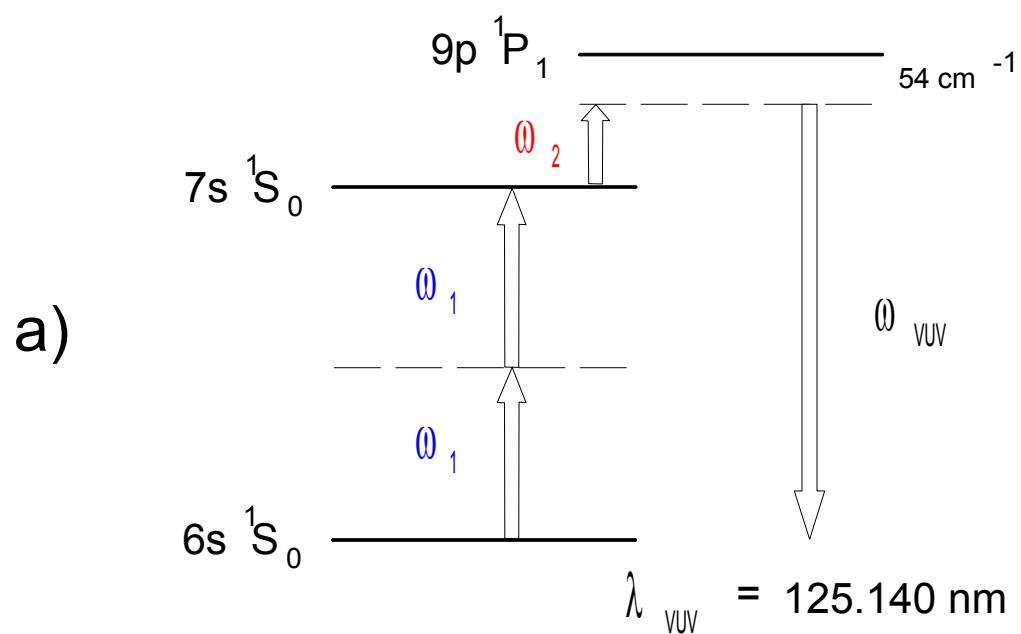
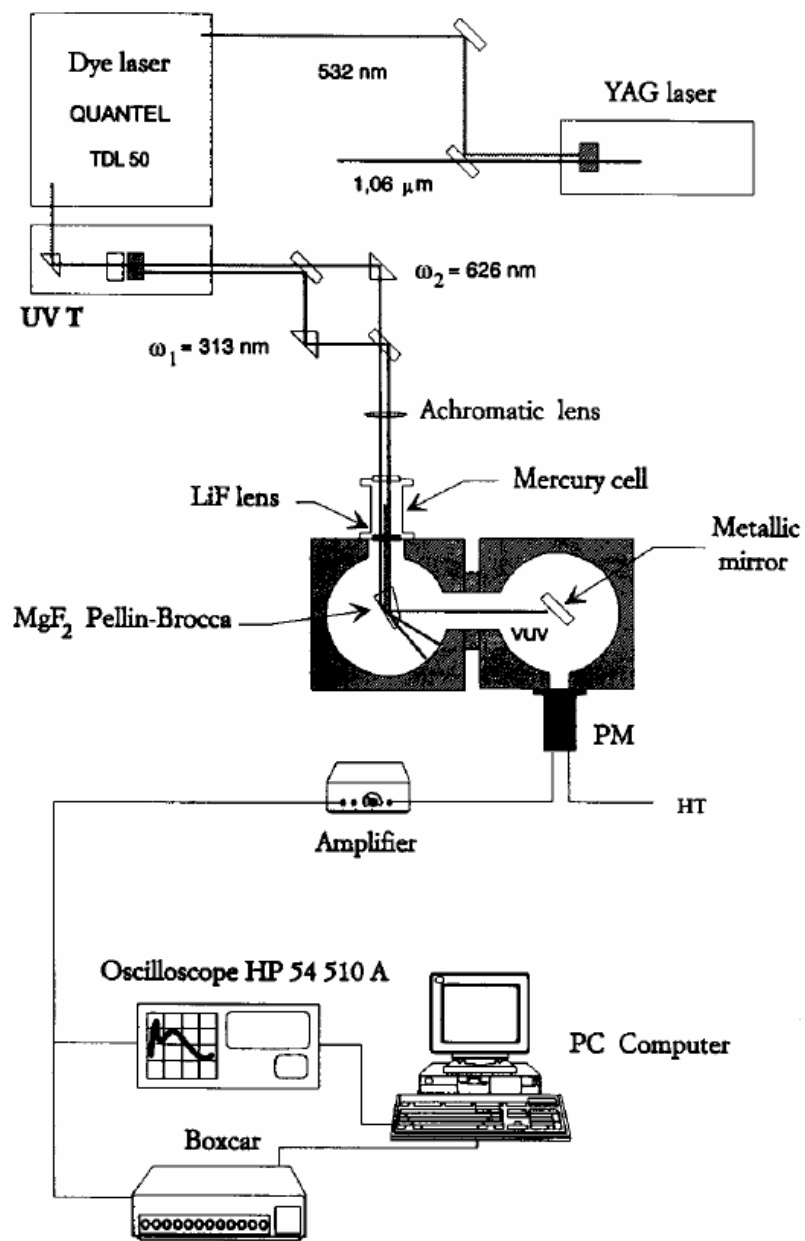


Fig.1

Fig 2





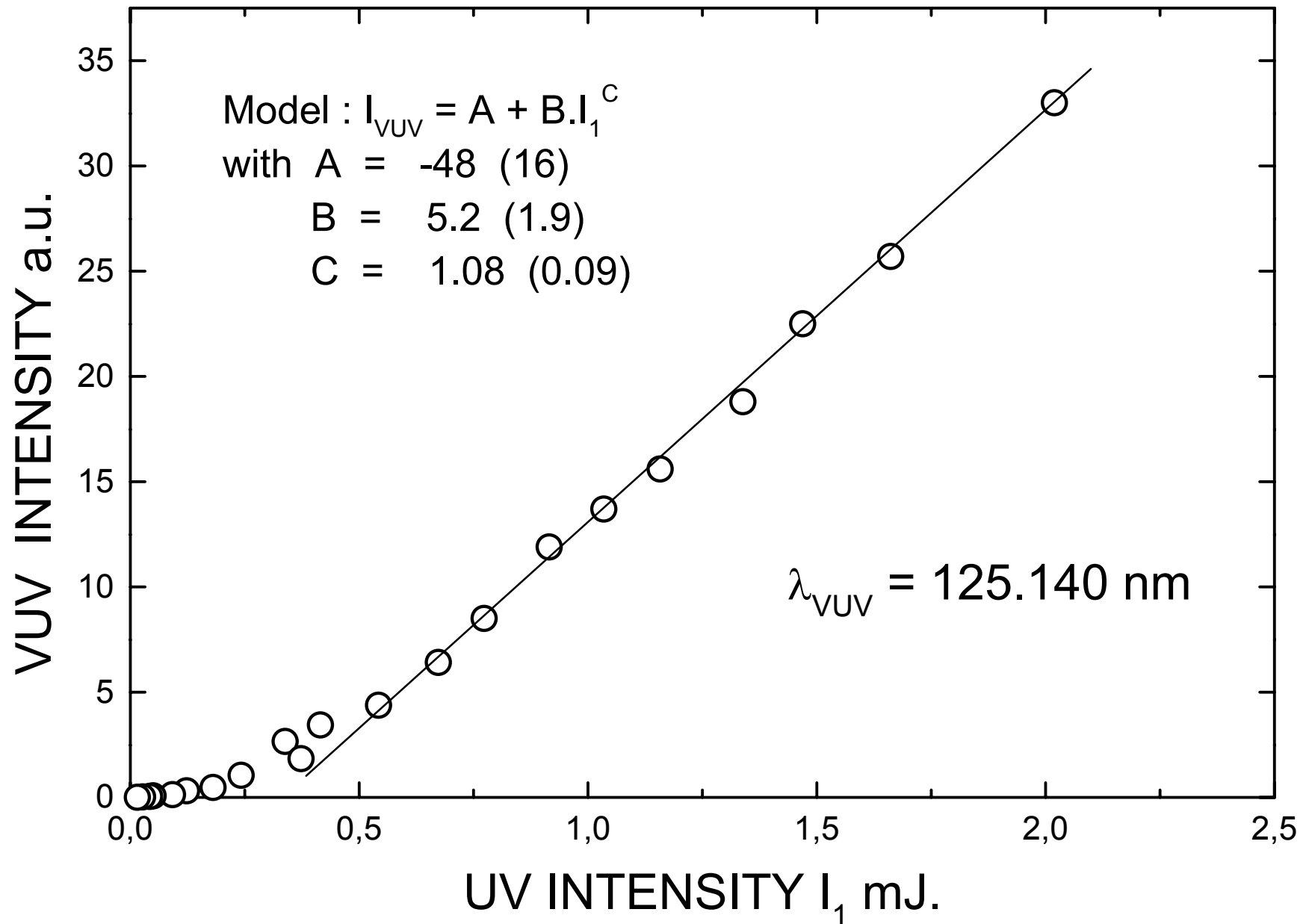


Fig.4

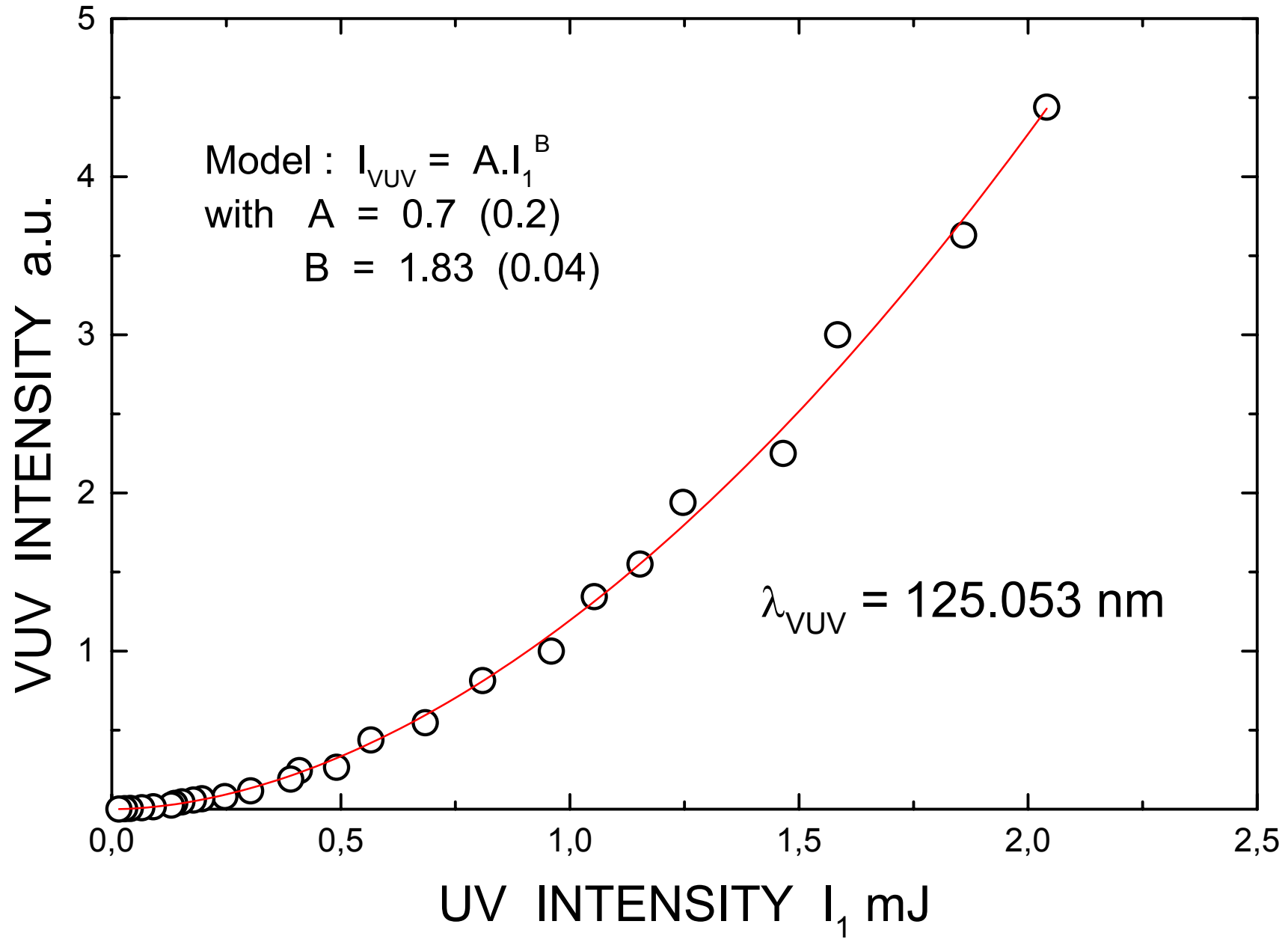


Fig.5

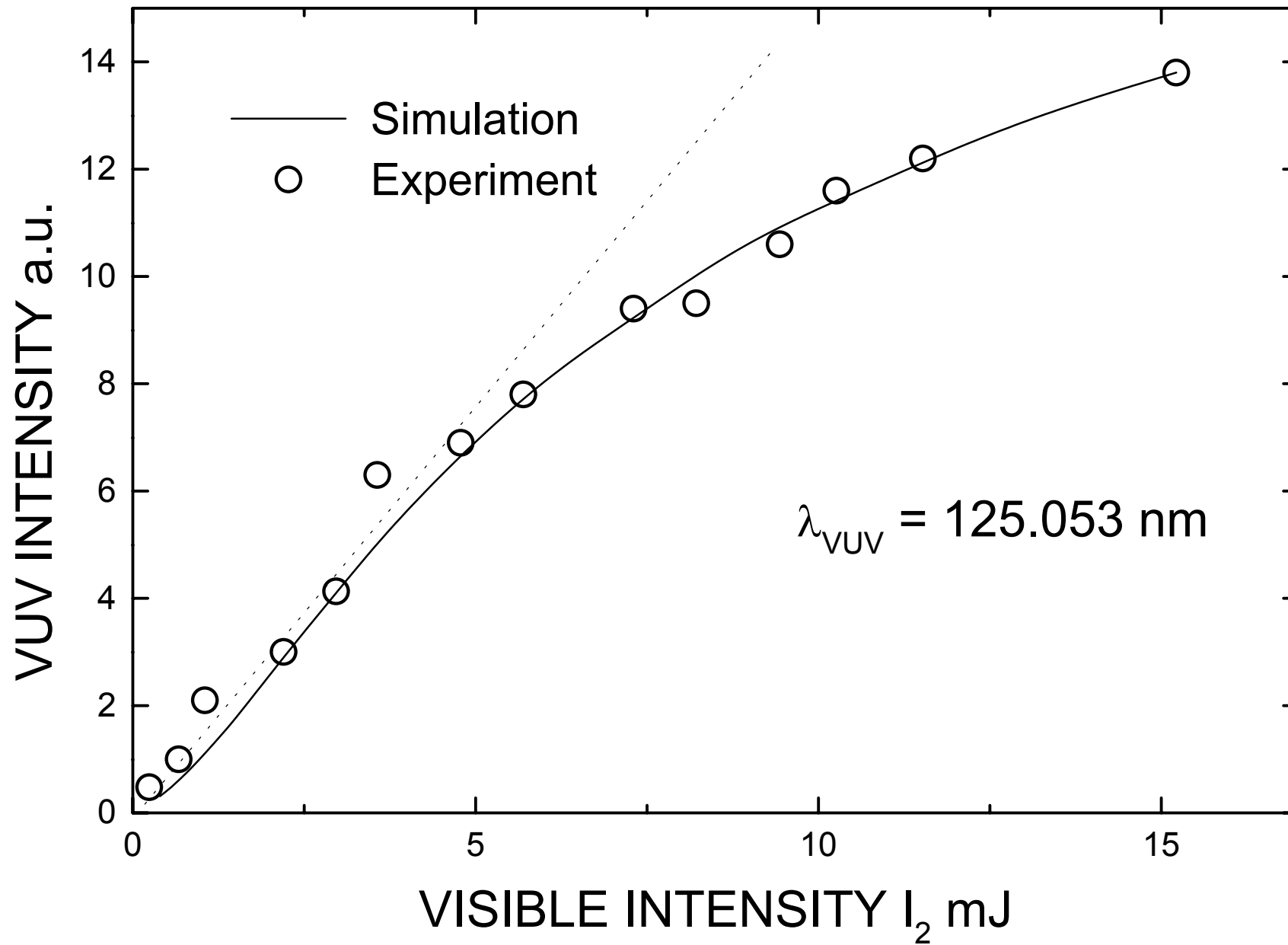


Fig.6

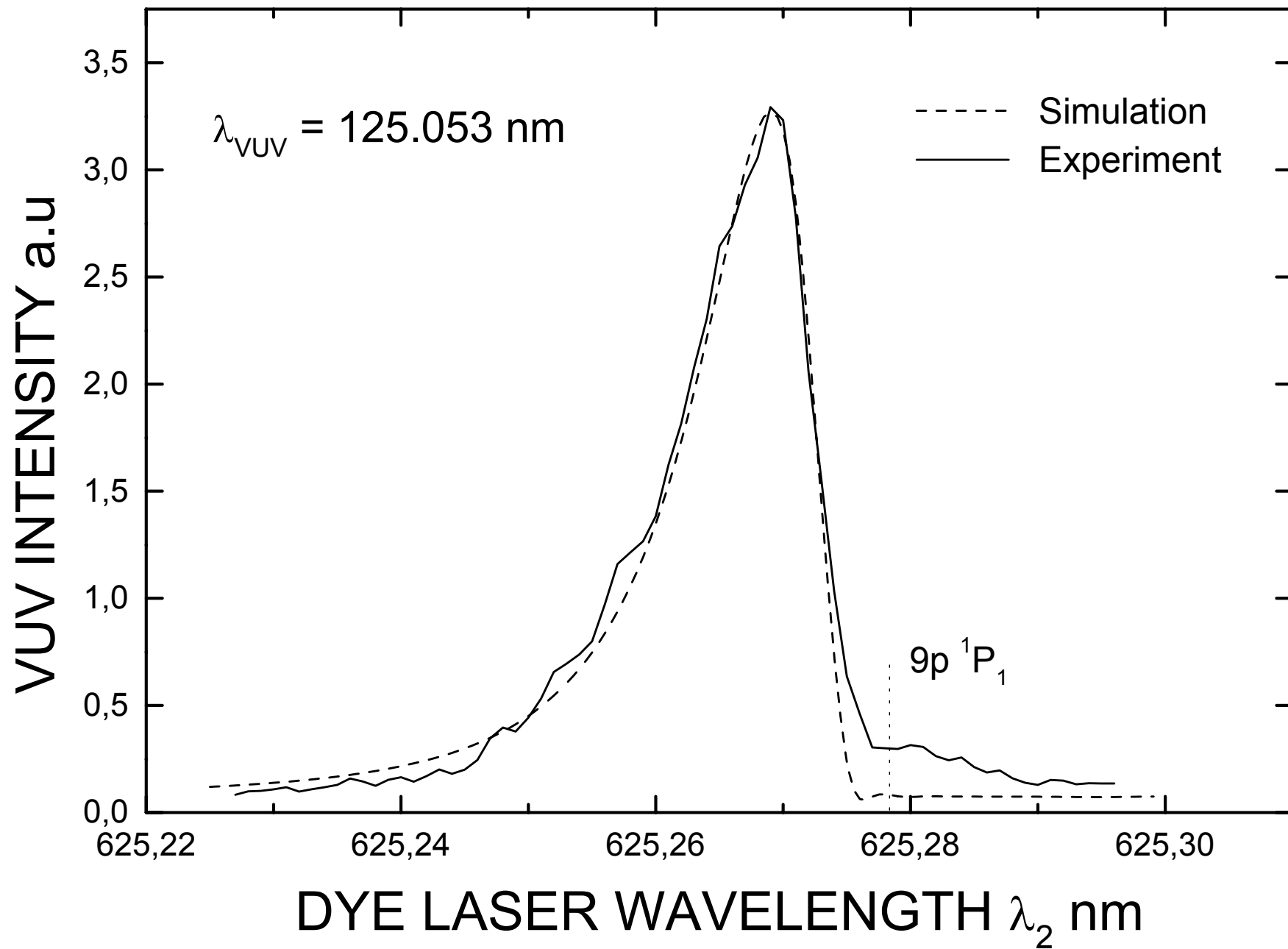


Fig. 7

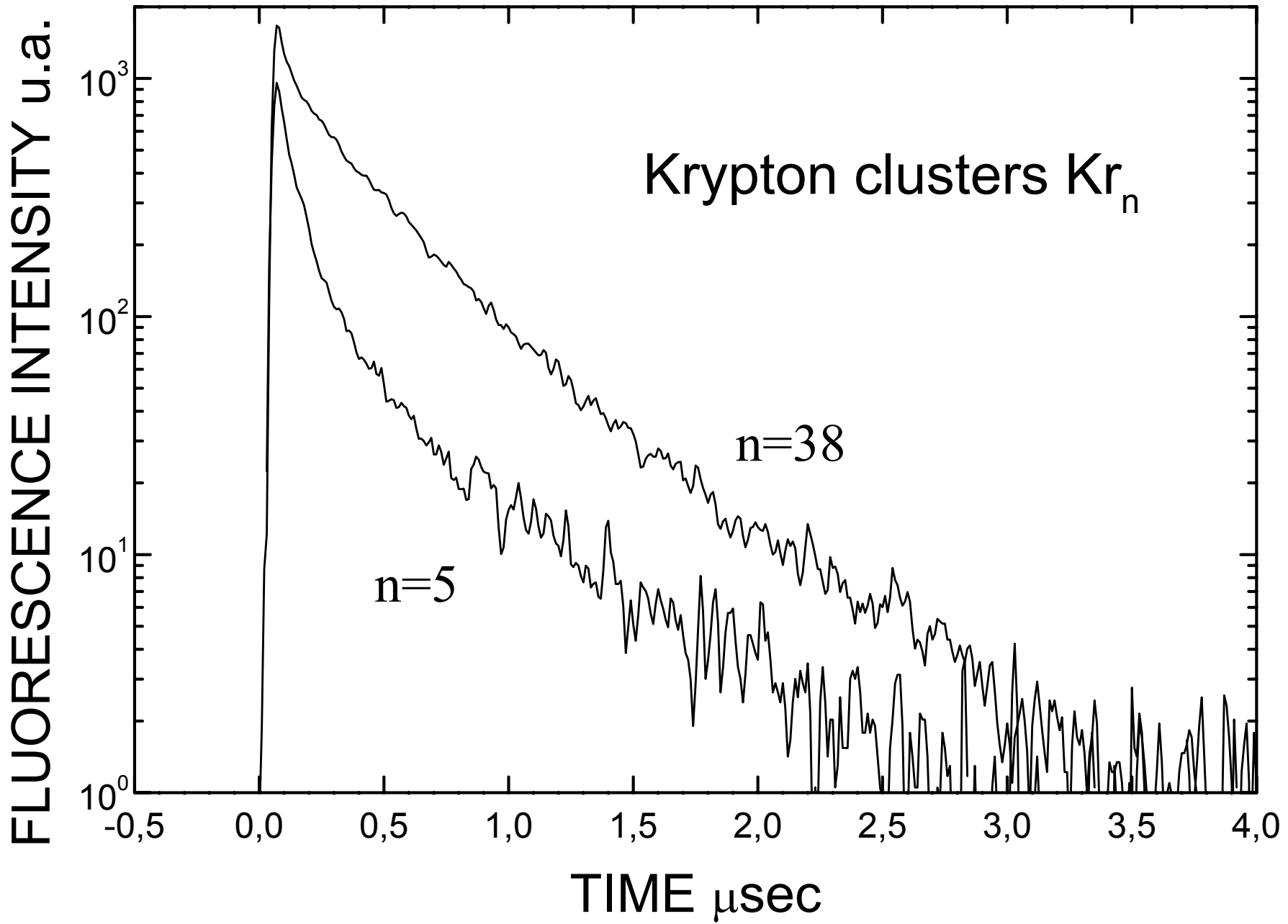


Fig.8